



K_2CO_3 -loaded hydrotalcite: A promising heterogeneous solid base catalyst for biolubricant base oil production from waste cooking oils



Guo Sun ^{a,b,1}, Ying Li ^{a,b,1}, Zizhe Cai ^c, Yinglai Teng ^{a,b}, Yong Wang ^{a,b,*}, Martin J.T. Reaney ^d

^a Guangdong Saskatchewan Oilseed Joint Laboratory, Department of Food Science and Engineering, Jinan University, Guangzhou 510632, China

^b Guangdong Engineering Technology Research Center for Oils and Fats Biorefinery, Guangzhou 510632, China

^c School of Pharmaceutical Sciences, Sun Yat-Sen University, Guangzhou 510006, China

^d University of Saskatchewan, Department of Plant Science, Saskatoon, SK S7N 5A8, Canada

ARTICLE INFO

Article history:

Received 29 November 2016

Received in revised form 23 February 2017

Accepted 28 February 2017

Available online 1 March 2017

Keywords:

Hydrotalcite/ K_2CO_3 heterogeneous catalyst

Trimethylolpropane fatty acid triester

Biolubricant base oil

Characterization

Recycling

ABSTRACT

Hydrotalcite (HT) loaded with potassium carbonate (K_2CO_3) was originally applied as a promising heterogeneous solid base catalyst for the production of trimethylolpropane fatty acid triester (TFATE) as the biolubricant base oil through transesterification of fatty acid methyl esters (FAME) from waste cooking oils and trimethylolpropane (TMP), in which FAME to TMP ratio (3:1), catalyst dosage (2% w/w), pressure (300 Pa), temperature (160 °C) and time (2 h) were optimized in order to obtain the best TFATE yield (80.6%). Based on the above, K_2CO_3 dosage (30% w/w) and calcination temperature (500 °C) in the preparation of HT/ K_2CO_3 catalyst were optimized to improve the TFATE yield to 93.9% along with 97.7% of conversion rate of FAME (CRF). The catalyst recycling was also investigated to determine the suitable reactivated method. Besides, HT/ K_2CO_3 catalysts in various states were characterized for better comprehension of their functional mechanisms and appropriate potential applications.

© 2017 Elsevier B.V. All rights reserved.

1. Introduction

For continuous environmental deterioration caused by the leakage of mineral-based lubricants, the worldwide requirement for sustainable development and eco-friendly products are currently on the rise [1]. As the Global Industry Analysts estimated [2], the global aggregate demand of lubricants will reach 4.13 hm³ by 2017. Hence, it is inevitable to employ bio-based oils instead of mineral ones which account for 85–90% of global lubricant base oils produced every year. Although biolubricant like vegetable oils can be used as either an alternative with almost the same function in the machine protection or biolubricant base oils, the higher production cost is the main bottleneck for its development compared to conventional lubricants [3,4]. Moreover, there are other four types of biolubricant base oils including polyalphaolefins, polyalkylene glycols, dibasic acid esters and polyol ester [5], among which trimethylolpropane fatty acid triester (TFATE) as a type of polyol

ester has proved to be a potential biolubricant base stock due to its favorable lubricity, stability, biodegradability and physicochemical properties, as compared to another pentaerythritol fatty ester [6,7]. Furthermore, the transesterification of fatty acid methyl ester (FAME) and trimethylolpropane (TMP) was reportedly preferred to the esterification of free fatty acids (FFA) with TMP because of its low cost, energy efficient and higher yield as well [8].

The transesterification catalyst for TFATE production was normally classified into enzyme, heterogeneous, homogeneous base and acid catalysts [9–12]. Thereinto, using less corrosive heterogeneous catalyst can not only eliminate procedures like neutralization and washing, but also can be recycled after simple filtration [13]. As previously reported, a range of heterogeneous base catalysts have been widely studied for biodiesel production [14–17]. Nevertheless, the preparation of such catalysts is relatively complicated involving high temperature and pressure in general [18,19]. Hydrotalcite (HT) is commonly a di-hydroxyl complex metal oxide possessing layered and porous structures, which can be recognized as catalyst carrier, ion-exchange and composite materials. HT loaded with potassium carbonate (HT/ K_2CO_3) had been discussed for improving the catalyst activity in biodiesel productions [20]. The calcination of HT/ K_2CO_3 at higher temperatures (≥ 400 °C) can decompose the carbonate into its metal oxide form, which generates highly dispersed active sites on the HT surface for various catalytic reactions. Nonetheless, such catalyst in biolubricant

* Corresponding author at: Guangdong Saskatchewan Oilseed Joint Laboratory, Department of Food Science and Engineering, Jinan University, Guangzhou 510632, China.

E-mail addresses: wangyjnu@hotmail.com, twyong@jnu.edu.cn (Y. Wang).

¹ Ying Li and Guo Sun contributed equally to this work and should be considered as co-first authors.

productions has rarely been studied, as well as its elaborate characterization, optimal preparation and recycling.

Considering the above, a thorough study of HT/K₂CO₃ reutilized for the production of TFATEs as biolubricant base oils was hereby provided using economically available waste cooking oils (WCO) in China as the feedstock. Firstly, a preliminary single-effect study for the TFATE production was conducted in terms of FAME to TMP ratio, catalyst dosage, reaction pressure, temperature and time. Subsequently, both the preparation and the recycling of HT/K₂CO₃ catalyst were optimized for obtaining desirable mass fraction of TFATE (MFT) and conversion rate of FAME (CRF). Regarding the characterization of HT/K₂CO₃ catalysts in various states, a series of modern methods were employed to expound the relationship between structural changes and catalytic activity concerning their catalytic active sites, microstructures, thermo-stability, metal ion leaching, specific surface areas, pore sizes and volumes for better comprehension of their functional mechanisms in future biolubricant base oil production.

2. Experimental

2.1. Materials

WCO with an acid value of 78.8 mg KOH/g and an initial moisture content of 0.6% from restaurants were provided by Balis Waste Treatment in Guangzhou, China, in which remaining food and water were removed by filtration after settling. The main components in WCO were FFA (38.7%), diacylglycerol (5.4%) and triacylglycerol (55.9%). TMP was obtained from Keoumi Chemical Reagent in Tianjin, China. Solid superacid of sulfated zirconia supported alumina (SO₄²⁻/ZrO²⁻:Al₂O₃) was purchased from Taide Chemical Scientific in Shandong, China. HT was supplied by Tiantang Chemical in Hunan, China. K₂CO₃ (>99%) and all other chemical reagents were of analytical grade from Fuyu Chemical in Tianjin, China.

2.2. HT/K₂CO₃ preparation and optimization

The HT/K₂CO₃ catalyst was prepared according to our developed method [21]. On one hand, 25 g of HT and 5 g of K₂CO₃ were mixed with 100 mL of distilled water in a flask of 250 mL for 24 h reaction at 80 °C, in which agitation was implemented for the first hour only. The resultant slurry was then oven dried at 80 °C for 5 h, followed by grinding and calcination at 600 °C for 6 h to form the solid base catalyst for the single factor experiment in the following transesterifications. On the other hand, different K₂CO₃ dosages (15, 20, 25 and 30%) and calcination temperatures (400, 500, 600 and 700 °C) were characterized based on the optimal conditions from single-factor experiments above, in which 100 mL of distilled water was poured into 50 g of HT/K₂CO₃ mixture instead here.

2.3. HT/K₂CO₃ characterization

HT/K₂CO₃ catalysts in various states were firstly pressed into KBr pellets for a qualitative Fourier Transform infrared spectroscopy (FT-IR), in which the spectra were recorded over 32 scans by a 640-IR spectrometer (Varian, USA) in a transmission mode from 4000 to 400 cm⁻¹ with a resolution of 1 cm⁻¹. X-ray diffraction (XRD) was then conducted using an MSAL XD-II X-ray diffractometer from Persee in Beijing, China with Cu K α radiation ($\lambda = 0.15418$ nm). All samples were measured at 36 kV and 20 mA scanning from 10 to 80° at 4°/min. Thermogravimetry/differential thermal analysis (TG-DTA) was carried out on the samples heating up to 950 °C at 10 °C/min in an air flow with a Mettler Toledo TGA/SDTA85 from USA. The microstructure was observed by an ULTRA-55 field emission scanning electron microscope (FESEM) from ZEISS, Germany at a magnification of 20000 \times . The property of HT/K₂CO₃ was also

measured by an automatic specific surface area/pore size distribution analyzer (BET sorp-mini II, ASAP010 Micromeritics instrument, USA), which was purged with helium gas during operation. The isotherms were generated by sweeping nitrogen onto the catalysts in a bath containing liquid nitrogen at 77 K. The relative pressure range was set at 2–99 kPa for adsorption and 97–31 kPa for desorption.

2.4. HT/K₂CO₃ application for TFATE production using WCO

The pathway of TFATE production (Fig. 1) starts with the production of WCO-FAME via a two-step process [22]. Firstly, WCO was filtered to remove solid particles before the esterification with glycerol catalyzed by solid superacid to lower the content of free fatty acids. The catalyst was removed by filtration and the esterified WCO was then transesterified with methanol to produce crude FAME using the KOH catalyst. Methanol and water remaining in the crude FAME were vacuum evaporated (5000 Pa, 50 °C), before which the reaction product was washed with hot water (80 °C) twice to remove residual glycerol and soap. The prepared WCO-FAME was analyzed by GC-FID after and fractionated by a MD80 molecular distillation (MD) apparatus (Handway Technology, Foshan, China) equipped with a falling film evaporator (0.1 m²) and an internal condenser (0.05 m²). A jacketed glass vessel with a flow regulation valve was used to load the WCO-FAME into the MD equipment at 40 mL/h. The operating parameters were as follows: pressure (<0.1 Pa), wiped film speed (300 rpm), temperature for distillation, condensation and feeding tank was 140 °C, 50 °C and 110 °C, respectively. Distillates and residues were separately discharged into glass flasks by gravity, among which the purified WCO-FAME was added dropwise to the mixture of TMP and HT/K₂CO₃ catalyst for the TFATE production in a three-necked flask equipped with a condenser and a constant-pressure dropping funnel. This second transesterification was evaluated in terms of FAME to TMP molar ratio (2.5:1, 2.8:1, 3:1, 3.3:1 and 3.6:1), catalyst dosage (0.5, 1.0, 1.5, 2.0 and 2.5%, w/w), reaction pressure (100, 200, 300, 400, and 500 Pa), temperature (130, 140, 150, 160 and 170 °C) and time (1, 1.5, 2.0, 2.5 and 3 h) under the prescribed magnetic stirring of 300 rpm. After the reaction, the HT/K₂CO₃ catalyst simply filtrated from the TFATE product was recycled and the TFATE was collected for further analyses.

2.5. FAME and TFATE analysis

The composition of fatty acid and TMP esters was determined by an Agilent 7820A gas chromatography (Agilent Technologies, Palo Alto, USA) equipped with a flame ionization detector (FID) [23]. For FAME analysis, fatty acids were transmethylated to their methyl esters in GC-FID using a DB-wax capillary column (10 m × 0.1 mm × 0.2 μ m) with nitrogen as the carrier gas at a flow rate of 0.17 mL/min. The temperature of injector and detector was 240 °C. Samples were dissolved in hexane at a concentration of 10.0 mg/mL, 0.5 μ L of which was withdrawn and injected with a split ratio of 30:1. The oven temperature was programmed to increase from 100 to 220 °C at 100 °C/min, held at 220 °C for 2 min, then heated from 220 to 240 °C at 40 °C/min and maintained for 4 min at 240 °C.

For TFATE analysis, a DB-1HT capillary column (15 m × 0.25 mm × 0.1 μ m) was employed using nitrogen as the carrier gas at a flow rate of 4.41 mL/min. The temperature for injector and detector was 380 °C and 400 °C, respectively. The oven temperature was operated as follows: the initial temperature set at 50 °C was heated to 220 °C at 50 °C/min, then increased at 30 °C/min to 290 °C, then increased at 40 °C/min to 330 °C for 2 min interval and at 30 °C/min from 330 to 370 °C, held for another 3 min at 370 °C. Samples were dissolved in hexane at 10.0 mg/mL

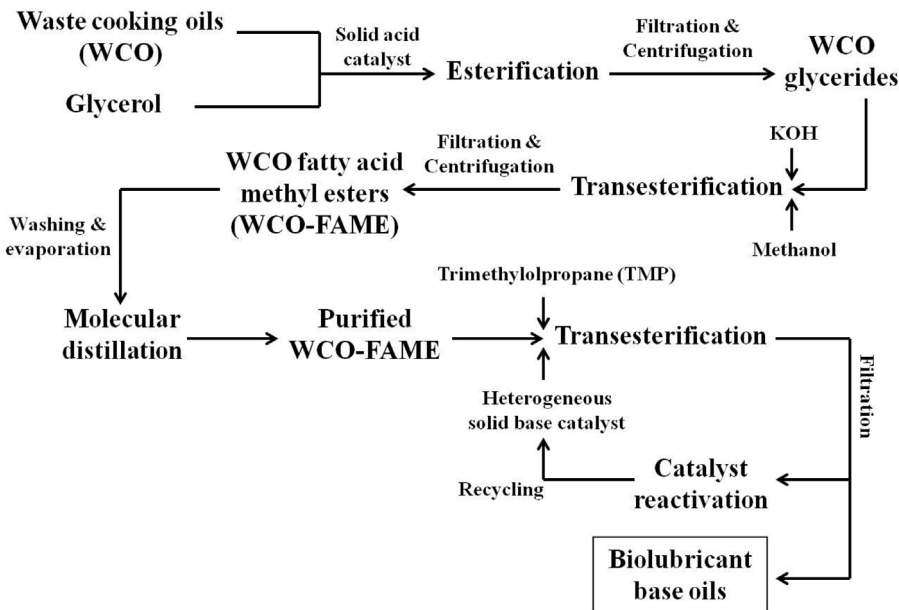


Fig. 1. Process diagram of biolubricant base oil production from waste cooking oils catalyzed by HT/K₂CO₃.

and 0.5 μ L of sample was injected with the split ratio of 20:1. Data were collected and processed with Agilent EZchrom Elite software. Both FAME and TFATE analytical results were expressed as relative percentages of the total fatty acid esters.

According to GC-FID results obtained, the mass fraction of TFATE (MFT) and the conversion rate of FAME (CRF) could be calculated as follows,

$$MFT (\%) = \frac{A_{tri}}{A_{tri} + A_{di} + A_{mono} + A_{FAME}} \times 100\% \quad (1)$$

where A_{tri} , A_{di} , A_{mono} and A_{FAME} are the peak area of TFATE, trimethylolpropane fatty acid diester (TFADE) and monoester (TFAME) and FAME, respectively.

$$CRF (\%) = \frac{\frac{R_{tri}}{M_{tri}} \times 3 + \frac{R_{di}}{M_{di}} \times 2 + \frac{R_{mono}}{M_{mono}}}{\frac{R_{tri}}{M_{tri}} \times 3 + \frac{R_{di}}{M_{di}} \times 2 + \frac{R_{mono}}{M_{mono}} + \frac{R_{FAME}}{M_{FAME}}} \times \frac{M}{3} \times k \times 100\% \quad (2)$$

where R_{tri} , R_{di} , R_{mono} and R_{FAME} indicate the mass fraction of TFATE, TFADE, TFAME and FAME, respectively. M specifies the molar ratio of FAME to TMP. k stands for the GC coefficient (1/1.1). M_{tri} , M_{di} , M_{mo} and M_{fame} represent the relative mass of TFATE, TFADE, TFAME and FAME in a sample, respectively [24].

2.6. Analysis of metal ion leaching

The metal ion leaching was traced by inductively coupled plasma-atomic emission spectrometry (ICP-AES) (Optima 2000DV ICP-AES, Perkin Elmer, USA). Samples were prepared at 160 °C for 2 h using FAME to TMP molar ratio (3.5:1) and catalyst dosage (2% w/w), which were carbonized and incinerated at 600 °C for 4 h. The ashed samples were dissolved in 5 mL of nitric acid and diluted to 50 mL with distilled water for analysis using the following conditions: 1.1 kW of forward power, 30 °C of oven temperature, 0.2 L/min for auxiliary gas flow rate, 15 L/min for nebulizer gas flow rate, 0.8 L/min for plasma gas flow rate and 1.5 mL/min for the pump sample quantity. All determinations were performed in triplicate.

2.7. Recycling of HT/K₂CO₃ catalyst

The recycling of HT/K₂CO₃ catalyst from vacuum filtration was investigated using five reactivated methods below:

- a Direct reuse;
- b Hexane treatment: 5.0 g of recovered HT/K₂CO₃ catalyst placed in a centrifuge tube of 50 mL was washed thrice with 50 mL of n-hexane, which was vacuum dried at 40 °C for 2 h to remove n-hexane, and then at 80 °C for 5 h to remove water;
- c Calcination after hexane treatment: HT/K₂CO₃ from the method above was calcinated in a muffle oven at 600 °C for 5 h;
- d Hexane and methanol treatment: HT/K₂CO₃ from the second method was washed with 50 mL of methanol in the centrifuge tube by vortex mixing to eliminate the formed soap within, which was then centrifuged at 2000 rpm and vacuum dried at 40 °C for 2 h to remove methanol and at 80 °C for 5 h to remove water;
- e Calcination after hexane treatment and impregnation: HT/K₂CO₃ from the second method was impregnated with a K₂CO₃ solution of 5%.

The resulting slurry was oven dried at 80 °C for 5 h and then calcinated in a muffle oven at 600 °C for 5 h. The efficiency of five reactivated catalysts for the TFATE production was assessed as compared to the new-made catalyst under the same transesterification conditions.

3. Results and discussion

3.1. The composition of FAME from WCO

As Table 1 represented, nine WCO-based FAMEs were characterized with 61.1% of unsaturation degree, which leads to desirable low-temperature properties and oxidative stability for producing TFATE as the base oil for biolubricant [1]. The three major components in the WCO-based FAME are methyl oleate (36.11 ± 1.58%), methyl palmitate (31.87 ± 1.10%) and methyl linoleate (21.71 ± 1.06%), which was consistent with the composition in the blend of soybean and palm oil [23]. The physicochemical property of TFATE depends largely on the fatty acid composition. The average molecular weight ($M_{average}$) of WCO FAME could be calculated as 286 Da in light of Eq. (3), which helps to determine the specific dosage of TMP used in the following transesterifications.

$$M_{average} = \frac{100}{\frac{m_1}{M_1} + \frac{m_2}{M_2} + \dots + \frac{m_x}{M_x}} \quad (3)$$

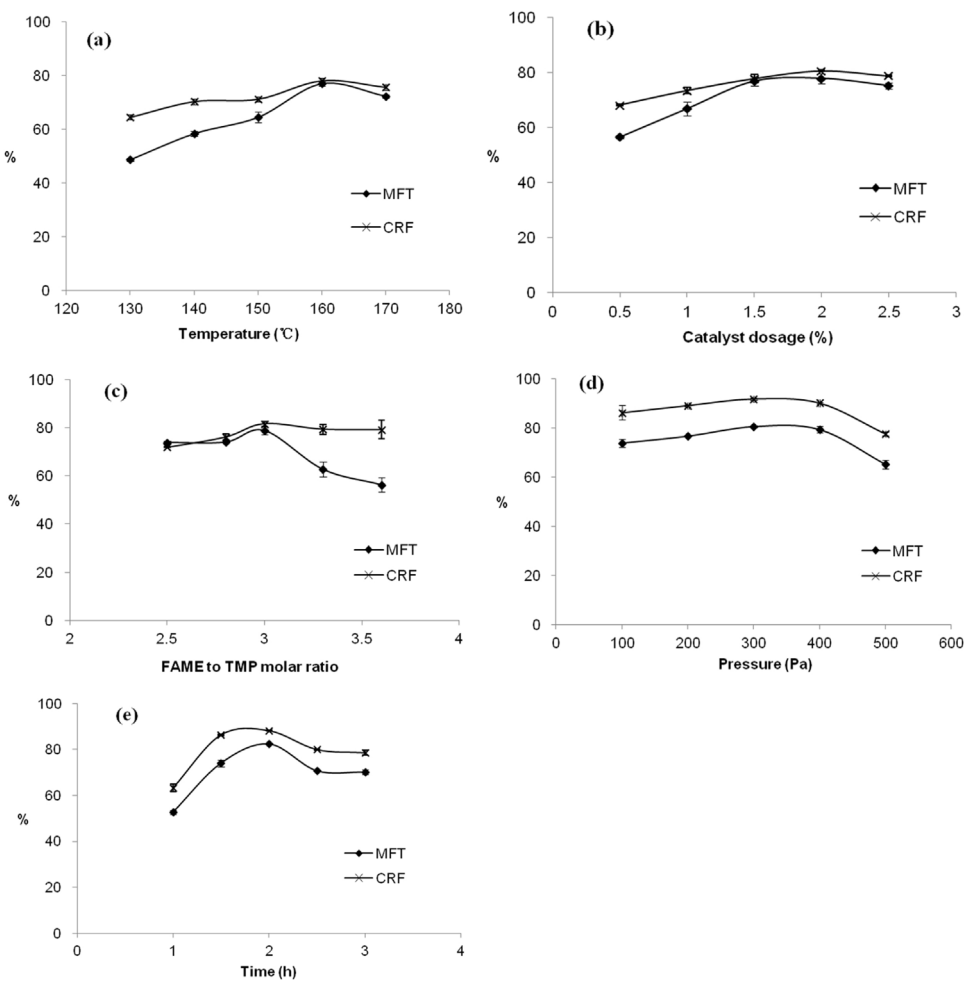


Fig. 2. The single effect of reaction parameters on mass fraction of trimethylolpropane fatty acid triester (MFT) and conversion rate of FAME (CRF): (a) temperature (FAME to TMP molar ratio: 2.8:1, catalyst dosage: 1.5% w/w, 400 Pa and 2 h); (b) catalyst dosage (160 °C, FAME to TMP molar ratio: 2.8:1, 400 Pa and 2 h); (c) FAME to TMP molar ratio (160 °C, catalyst dosage: 2% w/w, 400 Pa and 2 h); (d) pressure (160 °C, FAME to TMP molar ratio: 3:1, catalyst dosage: 2% w/w and 2 h); (e) time (160 °C, FAME to TMP molar ratio: 3:1, catalyst dosage: 2% w/w and 300 Pa).

Table 1
The composition of fatty acid methyl esters (FAME) transformed from waste cooking oils.

Retention time (min)	FAME	Relative content (%)
8.8	Methyl myristate	0.82 ± 0.08
10.9	Methyl palmitate	31.87 ± 1.10
11.1	Methyl palmitoleate	1.10 ± 0.11
12.8	Methyl stearate	6.19 ± 0.56
13.0	Methyl oleate	36.11 ± 1.58
13.6	Methyl linoleate	21.71 ± 1.06
14.2	Methyl linolenate	1.53 ± 0.35
14.8	Methyl arachidate	0.35 ± 0.03
15.0	Methyl eicosanoate	0.32 ± 0.01

Values are presented as means ± standard deviation of triplicate.

where X is nine, $m_{1,2,\dots,x}$ and $M_{1,2,\dots,x}$ stand for weight in 100 g of WCO-based FAME and molecular weight, respectively, corresponding to nine identified FAMEs.

3.2. The single-factor effect on the TFATE production

Fig. 2 illustrated earlier increase and later decrease trend for all five operating parameters in the HT/K₂CO₃-catalyzed transesterification of TMP and WCO-FAME. Temperature was investigated first while other reaction parameters were set as FAME to TMP molar ratio of 2.8:1, catalyst dosage of 1.5%, time of 2 h and pressure of

400 Pa. The upward trend of MFT was similar to that of previous study [25], but in this case, the MFT and CRF increased quickly to their peak at first ranging from 130 to 160 °C, followed by a slight decline as the temperature continued to increase (Fig. 2a). It is known that higher temperatures are preferred for the endothermic transesterification. However, the elevated temperatures may induce more TMP evaporation and side reactions like saponification and partial carbonization, which lead to a reduced TFATE yield and product quality. Thus, 160 °C was selected as the optimal temperature for subsequent reactions.

As shown in Fig. 2b, the increased catalyst dosage could accelerate the reaction, from which the highest MFT and CRF were obtained using 2% w/w of catalyst dosage and they gradually decreased afterwards. This may be due to the limited solubility of HT/K₂CO₃ in TMP and the lack of catalyst substrates. Considering the costing and the difficulty in post-treatments, 2.0% was considered the optimal catalyst dosage. MFT and CRF rose up to their maximum when FAME to TMP molar ratio of 3:1 was used in Fig. 2c. However, a further increase of FAME loading caused a sharp decline in the MFT, which could be explained by the excessive addition of FAME that adversely affected the reaction equilibrium in the TFATE synthesis. Moreover, the recovery of unreacted FAME would consume more energy and cost. Therefore, the FAME to TMP molar ratio of 3:1 was chosen.

A significant increase in MFT and CRF was found as the pressure decreased from 500 to 300 Pa (Fig. 2d). The further decrease of

pressure would let both FAME and TMP boil at a lower temperature, resulting in an evaporation loss of raw reactants required for the TFATE synthesis. Hence, 300 Pa was selected as the optimal. Time also had significant effect as it went up from 1 to 2 h. Both MFT and CRF dropped down afterwards but the extension of time had little effect on the further TFATE synthesis. Meanwhile, the prolonged time also require more energy. Consequently, 2 h has been used to ensure the efficiency of TFATE production.

According to the single-factor experimental results above, the operating parameters for subsequent experiments were determined with the consideration of both costing and efficiency. The highest MFT (82.5%) and CRF (88.2%) could be attained under the optimal conditions as follows: FAME to TMP molar ratio of 3:1, catalyst dosage of 2% w/w, 160 °C, 300 Pa and 2 h.

3.3. Optimization of prepared HT/K₂CO₃ catalyst

The preparation of HT/K₂CO₃ catalyst was optimized based on the optimal transesterification obtained before. As described in Table 2, the CRF kept rising at a constant calcination temperature (600 °C) as the K₂CO₃ dosage increased, in which an insignificant difference in the CRF change was found as the K₂CO₃ dosage increased from 15 to 25% whereas the CRF went dramatically up to its peak (87.1%) when the K₂CO₃ dosage reached 30%. The CRF change was significant when 30% of K₂CO₃ dosage was fixed at different calcination temperatures, among which 500 °C performed the best. Therefore, 30% of K₂CO₃ dosage at 500 °C of calcination temperature was determined for the preparation of HT/K₂CO₃ catalysts.

3.4. HT/K₂CO₃ characterization

3.4.1. FT-IR spectra

Owing to the stretching vibration of hydroxyls in the hydrated surface layer formed by water molecules [26], the absorbance ranging from 3800 to 3250 cm⁻¹ was observed, as well as a similar absorption around 3199.35 cm⁻¹ in the spectra of 400 °C. As illustrated in Fig. 3a, the band at about 3459.96 cm⁻¹ associated with stretching vibrations is due to the water absorption onto the surface of the catalyst, and it could also be partly attributed to the stretching vibration of the Al–O–K groups, which is considered to be active sites [27,28]. A δ-OH bending vibration at 1636.89 cm⁻¹ may be resulted in the water absorption from the air as well, which might also greatly affect the XRD spectra [29]. The absorbance of CO₃²⁻ bonding K⁺ was commonly in the range of 1722–1160 cm⁻¹ [30], in which the absorbance around 1477 cm⁻¹ could be attributed to the symmetric and asymmetric stretching vibrations of mono-dentate carbonates at the surface of the K₂CO₃ [31], and the HT/K₂CO₃ calcinate exhibited the co-existence of weak absorption peaks around 1410 cm⁻¹. Moreover, the absorption at 487 cm⁻¹ was probably caused by the lattice vibration of metal oxide (KO_x) [32]. In Fig. 3b, the absorption peaks of HT/K₂CO₃ calcinates at 500 °C were stronger as the K₂CO₃ dosage increased, and absorptions around 861 and 670 cm⁻¹ were found in all HT/K₂CO₃ calcinates, which could be assigned to the stretching vibration of Al–O active sites [33]. In the case of 30% of K₂CO₃ dosage used (Fig. 3c), the HT/K₂CO₃ calcinate at 500 °C gave a stronger absorption band around 1477 cm⁻¹ due to the presence of carbonate [25]. The absorption peaks around 3427 cm⁻¹ for higher calcination temperatures were very similar to hydroxy absorption band around 3412 cm⁻¹ reported for irreversible structures like KAl(CO₃)(OH)₂ and Mg(Al)O_x, which could also exhibit its absorptions at 1105 cm⁻¹ [34]. This means that irreversible structures generated at 600 or 700 °C could reduce the surface area and alkalinity of catalysts. Notwithstanding, no irreversible structures were found for HT/K₂CO₃ calcinated at 400 and 500 °C, in which incon-

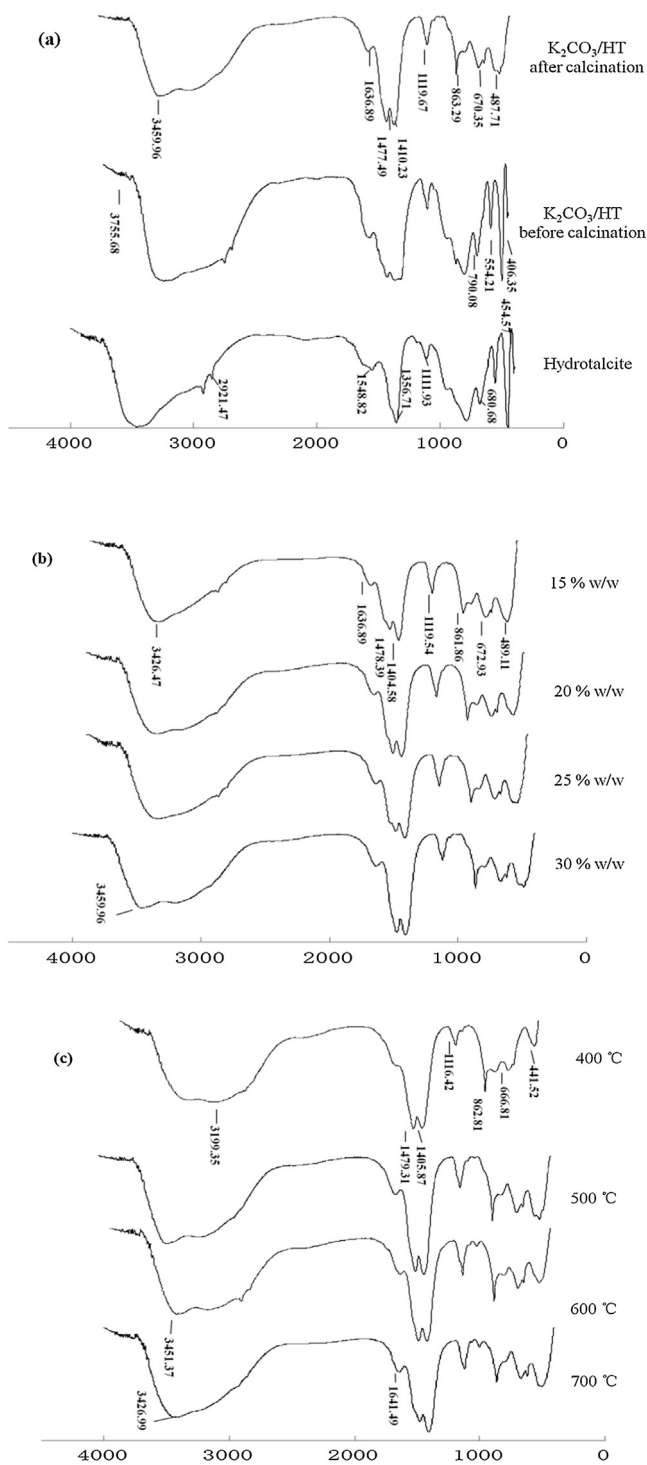


Fig. 3. FT-IR spectrum: (a) Hydrotalcite (HT), HT/K₂CO₃ before and after calcination; (b) HT/K₂CO₃ catalyst with different K₂CO₃ dosages at the calcination temperature of 600 °C; (c) HT/K₂CO₃ catalyst with the K₂CO₃ dosage of 30% w/w under different calcination temperatures.

spicuous absorption peaks around 860 and 670 cm⁻¹ indicated less active sites on the HT/K₂CO₃ calcinated at 400 °C. Based on the above, it could be concluded that only calcination induced the formation of active sites (i.e., K and Al oxides) on the HT/K₂CO₃, in which one with 30% of K₂CO₃ addition at 500 °C calcination seems to have better characteristic peaks in accordance with the obtained optimal conditions for the HT/K₂CO₃ preparation.

Table 2

The performance of HT/K₂CO₃ catalyst under various conditions regarding the yield of trimethylolpropane fatty acid mono-, di-, tri- esters and the conversion rate of FAME (CRF).

Preparation condition	TFAME ^a	TFADE ^b	TFATE ^c	CRF ^d
15% K ₂ CO ₃ at 600 °C	0.16 ± 0.28	7.75 ± 0.13	68.42 ± 0.54	76.53 ± 0.37
20% K ₂ CO ₃ at 600 °C	0.12 ± 0.21	2.94 ± 0.17	75.82 ± 1.48	79.25 ± 1.60
25% K ₂ CO ₃ at 600 °C	0.00 ± 0.00	2.00 ± 0.08	77.78 ± 0.57	80.20 ± 0.66
30% K ₂ CO ₃ at 600 °C	0.00 ± 0.00	2.09 ± 0.03	84.32 ± 0.44	87.12 ± 0.47
30% K ₂ CO ₃ at 400 °C	0.00 ± 0.00	6.72 ± 0.46	77.02 ± 2.66	84.29 ± 3.20
30% K ₂ CO ₃ at 500 °C	0.00 ± 0.00	2.58 ± 0.22	93.89 ± 0.44	97.71 ± 0.49
30% K ₂ CO ₃ at 700 °C	0.00 ± 0.00	4.52 ± 0.13	78.88 ± 0.03	83.95 ± 0.12

Values are presented as means ± standard deviation of triplicate.

^a TFAME: trimethylolpropane fatty acid monoester.

^b TFADE: trimethylolpropane fatty acid diester.

^c TFATE: trimethylolpropane fatty acid trimester.

^d CRF: conversion rate of FAME.

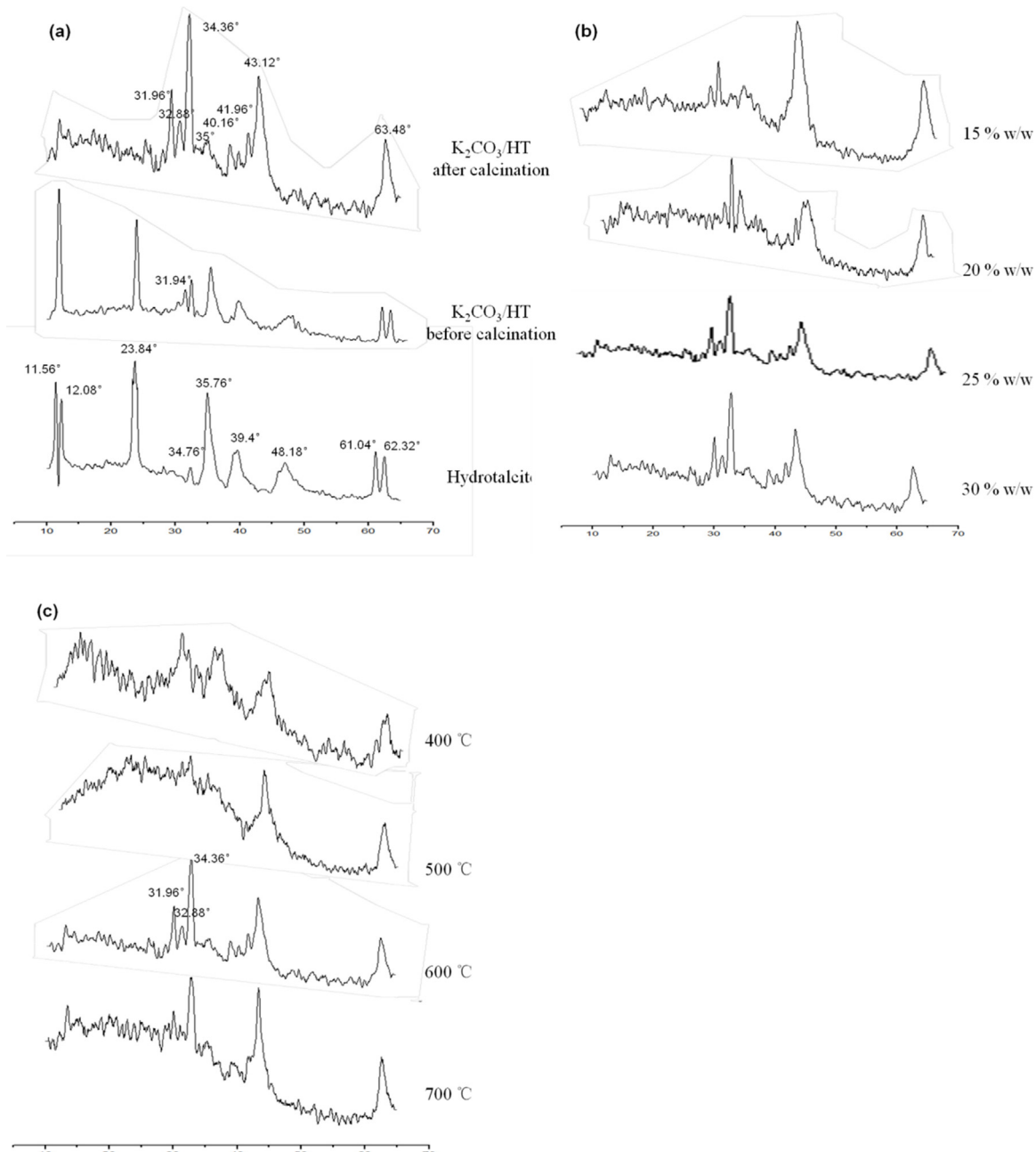


Fig. 4. X-ray diffractogram: (a) HT, HT/K₂CO₃ before and after calcination; (b) HT/K₂CO₃ catalyst with different K₂CO₃ dosages at the calcination temperature of 600 °C; (c) HT/K₂CO₃ catalyst with the K₂CO₃ dosage of 30% w/w under different calcination temperatures.

3.4.2. XRD diffractograms

As can be seen in Fig. 4a, the XRD diffraction pattern of HT displayed typical characteristic peaks at 11.56° , 12.08° , 23.84° , 34.76° , 35.76° , 39.4° , 48.18° , 61.04° and 62.32° [35], among which the peaks at 11.56° and 23.84° could be used to calculate the basal spacing between the layers whilst the peak at 61.04° could be used for calculating the unit-cell dimension [36]. However, the peaks at 11.56° and 12.08° were replaced by a new peak at 11.96° when adding K_2CO_3 into HT, as well as the new peak at 31.94° instead of the peak at 34.76° , indicating the layered basal spacing changed. After calcination, the HT layered structure was destroyed, and the characteristic peaks at 31.96° , 32.88° , 34.36° , 35° , 40.16° , 41.96° , 43.12° and 63.48° were exhibited [33], in which $Al-O-K$ ($2\theta = 43^\circ$) and K_2O ($2\theta = 63^\circ$) active sites were observed corresponding to their FT-IR absorbance [37,38]. These newly-formed crystals consisting of multiple metal oxides may explain the excellent catalytic activity of HT/K_2CO_3 . The XRD diffractogram of HT/K_2CO_3 calcinates with different K_2CO_3 dosages at $600^\circ C$ showed no significant difference in Fig. 4b whereas HT/K_2CO_3 calcinates at 600 and $700^\circ C$ with K_2CO_3 dosage of 30% presented the characteristic peaks at 31.99° , 32.88° , 34.36° in Fig. 4c corresponding to spinelle-like irreversible structures, which is in consistency with FT-IR spectra.

3.4.3. Thermal analysis

HT/K_2CO_3 before and after calcination ranging from 0 – $950^\circ C$ was traced by TG-DTA. Before calcination (Fig. 5a), endothermic peaks at about 75 and $110^\circ C$ were found accompanying with a total mass loss of 6.23% , which may be because of the elimi-

Table 3

The property of HT/K_2CO_3 catalysts prepared under different conditions.

Preparation condition	Special surface area (m^2/g)	Average pore size (nm)	Total pore volume (cm^3/g)
15% K_2CO_3 at $600^\circ C$	4.15	327.76	4.25
30% K_2CO_3 at $600^\circ C$	16.58	38.80	16.16
30% K_2CO_3 at $500^\circ C$	24.69	35.18	23.96

nation of interlayer and weakly bound water on the surface of MgO structures without disruptions [39]. The endothermic peak at around $230^\circ C$ involving a mass loss of 11.77% was attributed to the K_2CO_3 decomposition, which might lead to the carbonate ion and further decomposition in the brucite-like layers [40]. The mass loss of approximately 21.62% ranging from 300 to $510^\circ C$ was caused by the K_2O decomposition resulting in the anionic hydroxyls between brucite-like layers [27], in which the endothermic peak at around $450^\circ C$ represented the formation of K_2O and $Al-O-K$ during the K_2CO_3 decomposition as the main active sites required for the transesterification [41]. The last mass loss of 10.13% happened in the range of 510 – $900^\circ C$, suggesting the newly-formed substances in line with both FT-IR and XRD results. The catalytic activity decreased since K_2O species and $Al-O-K$ groups began to decompose when the calcination temperature increased over $510^\circ C$ [42]. HT/K_2CO_3 after calcination performed a good thermostability (Fig. 5b), in which the mass loss of 18.67% occurred only throughout the whole temperature range, corresponding to the loss of surface moisture.

3.4.4. BET analysis

BET special surface area is recognized an important characterization of solid catalysts due to its direct relation to the catalytic activity. In Table 3, the prepared HT/K_2CO_3 catalyst under optimal conditions had a special surface area of $24.69 m^2/g$ with an average pore size of $35.18 nm$ corresponding to mesoporous ($250 nm$), which could have a better catalytic efficiency for absorbing organic macromolecules in transesterifications [43]. As the calcination temperature rose up to $600^\circ C$, both special surface area and pore volume dramatically decreased due to the generation of metal oxides, which accords with IR, XRD and TG-DTG results. Such significant decline was also observed as the K_2CO_3 dosage decreased.

3.4.5. FESEM micrographs

The surface of HT appeared as a smooth laminated structure before and after adding K_2CO_3 (Fig. 6a, b) whereas the double-layered structures were significantly changed after calcination with numerous pores and spiculate substances on the surface (Fig. 6c). These typical needle/pillar-like structures are different from clustered spinel-like oxides formed on the calcined HT without the impregnation of metal carbonates [44], which are potential active sites or irreversible structures caused by excessive calcinations in accordance with FT-IR, XRD and TG-DTG results. On the whole, the larger special surface area and pore volume of HT/K_2CO_3 prepared under optimal conditions could improve the K^+ absorption onto the HT surface, which helped to enhance alkalinity and catalytic active sites [20]. The layered porous structure could also increase the contact area between catalysts and reactants in the catalysis. However, such structure got looser with an increased pore number as the calcination temperature rose up. The HT/K_2CO_3 calcinated at $700^\circ C$ presented a large number of compact spiculate structures on its surface due to the excessive calcinations, which led to the reduction of specific surface area closely related to the catalytic efficiency. The increasing K_2CO_3 dosage could also increase the number of pores and active sites on the HT/K_2CO_3 surface resulting in the higher

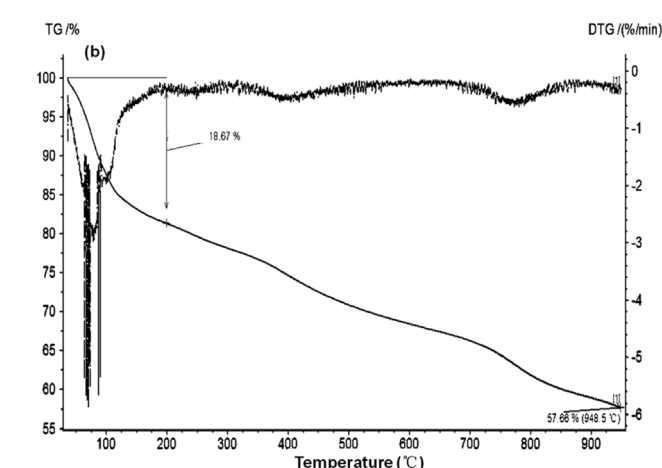


Fig. 5. Thermogravimetry/differential thermal analytical results for HT/K_2CO_3 catalysts: (a) before calcination; (b) after calcination.

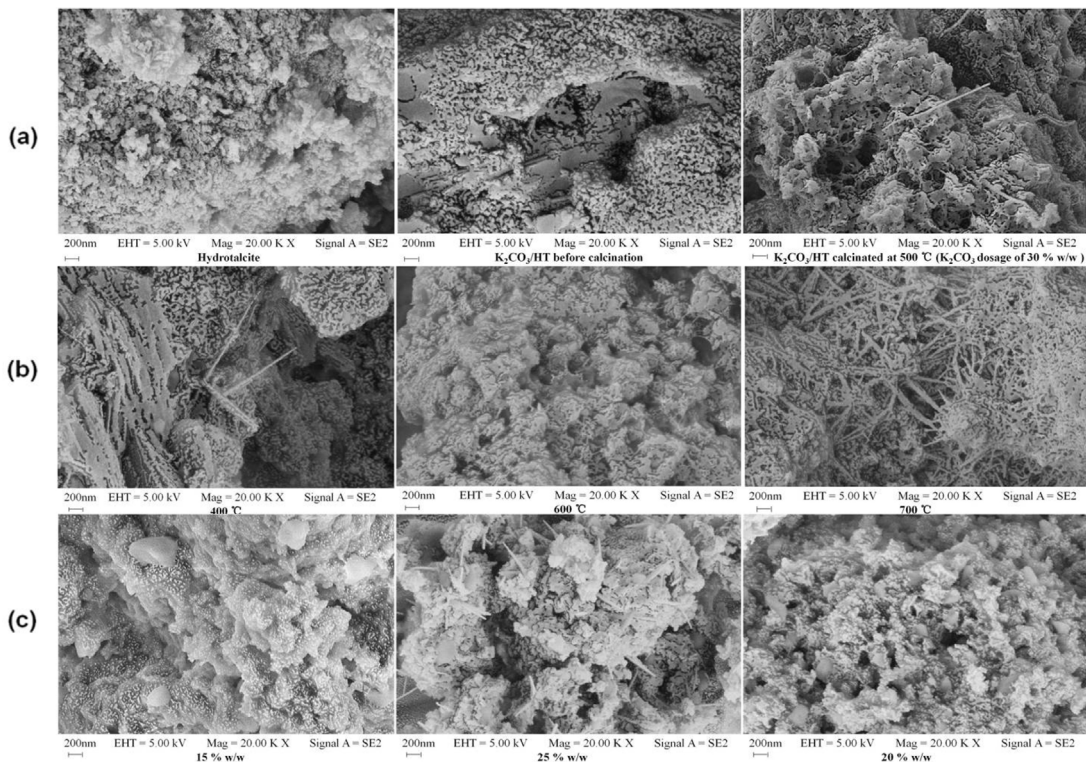


Fig. 6. Field emission scanning electron micrograph: (a) HT, HT/K₂CO₃ before and after calcination; (b) HT/K₂CO₃ catalyst with K₂CO₃ dosage of 30% w/w under different calcination temperatures; (c) HT/K₂CO₃ catalyst with different K₂CO₃ dosages at the calcination temperature of 600 °C.

MFT and CRF. Nonetheless, the HT/K₂CO₃ surface began to appear spiculate structures when K₂CO₃ dosage was beyond 25%.

3.4.6. Metal ion leaching in the TFATE

The metal ion leaching of the HT/K₂CO₃ in the TFATE, potassium ion in particular, increased certainly as the K₂CO₃ dosage increased from 25 to 30% when the calcination temperature was fixed at 600 °C (Table 4). However, this ion leaching significantly decreased since the HT/K₂CO₃ catalyst prepared under optimal conditions. In the case of fixed K₂CO₃ dosage (30%), potassium ion immediately dropped from 177.4 at 600 °C to 26.9 mg/L at 500 °C, which accounts for 2.7% of total potassium ions in the HT/K₂CO₃ catalyst. As previously mentioned, potassium leaching was relevant to the hydroxyl in methanol and the solubility of potassium ion increased with the number of alcohol groups [30,43]. Hence, the dissolution of potas-

Table 4

The content of metal ions in the trimethylolpropane fatty acid trimers (TFATE).

	K ⁺	Mg ²⁺	Al ³⁺	Na ⁺
25% K ₂ CO ₃ at 600 °C	131.90 ± 0.47	54.70 ± 0.31	11.30 ± 0.28	7.49 ± 0.11
30% K ₂ CO ₃ at 600 °C	177.40 ± 0.68	69.60 ± 0.42	10.60 ± 0.33	8.61 ± 0.15
30% K ₂ CO ₃ at 500 °C	26.92 ± 0.13	3.60 ± 0.10	0.31 ± 0.07	0.78 ± 0.02

Values are presented as means ± standard deviation of triplicate.

sium ions in TMP with three hydroxyl groups is easier than that in methanol. As compared to the conventional transesterification of triglyceride with methanol, the cleaner transesterification of TMP with FAME is less destructive to catalytic active sites thus resulting in reduced ion leaching.

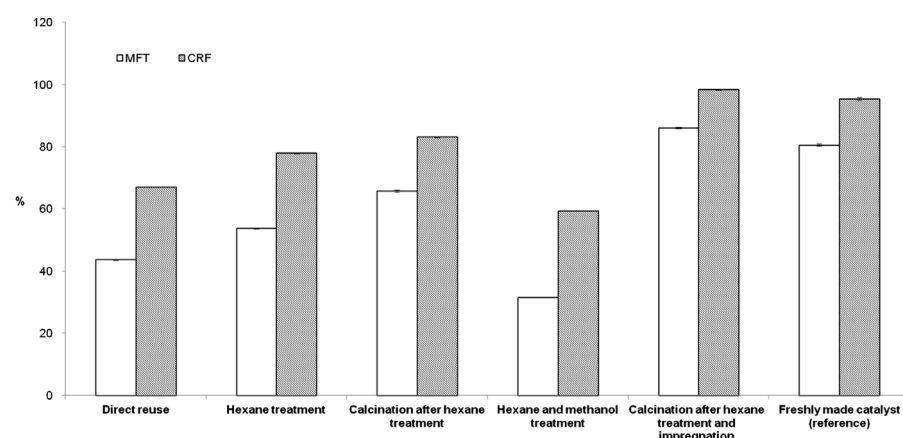


Fig. 7. The effect of different reactivation methods on the efficiency of recycled HT/K₂CO₃ catalyst regarding mass fraction of trimethylolpropane fatty acid triester (MFT) and conversion rate of fatty acid methyl ester (CRF).

3.5. Recycling of HT/K₂CO₃ catalysts

As depicted in Fig. 7, the HT/K₂CO₃ catalyst after hexane treatment obtained 10.89% higher CRF than direct reuse of the recycled catalysts, in which residual TFATE and soap could block catalytic active sites. The calcinated recycled catalyst after hexane treatment increased the CRF by 5.16% as compared to that without calcination. The high-temperature calcination could not only eliminate side products and water that negatively affect the catalyst, but also reactivate the active sites so as to increase the catalytic efficiency. The recycled catalyst after hexane and methanol treatment had the poorest MFT and CRF that may attribute to more potassium leaching caused by methanol washing, residual water in methanol, CO₂ and moisture reacted with KHCO₃ [30,42]. The catalyst reactivated by impregnation and calcinations after hexane treatment performed the best overall with MFT of 86.12% and CRF of 98.4%, which was even better than freshly made catalyst. This could be explained by the fact that the impregnation of more K₂CO₃ to the HT with some remaining active sites after hexane washing implies the formation of more catalytic active sites after calcination. For reactivation by calcinating the washed catalyst, the MFT increased from 22.21 to 42.58% in comparison with the reactivated catalysts by washing only without calcination (10.13%).

4. Conclusion

HT/K₂CO₃ catalyst, prepared with 30% of K₂CO₃ dosage at 500 °C under the optimal transesterification conditions, has been proved as a promising heterogeneous solid base catalyst for biolubricant base oil production from waste cooking oils accompanying with the highest MFT (93.9%) and CRF (97.7%) and the lowest potassium leaching. Furthermore, active sites and irreversible structures on the surface of HT/K₂CO₃ catalysts in various states were characterized for better understanding the catalytic mechanism. Besides, calcination was investigated to be necessary to reactivate catalysts for obtaining a satisfactory recycling.

Conflict of interest

The authors have declared no conflict of interest.

Acknowledgements

This work was supported by the Program for New Century Excellent Talents in University (Grant NECT-12-0675), Guangdong Provincial Department of Science and Technology (Grant 2012A03230016 and 2012B050600005) and the Fundamental Research Funds for the Central Universities (Grant 21612434).

References

- S.Z. Erhan, B.K. Sharma, Z. Liu, A. Adhvaryu, Lubricant base stock potential of chemically modified vegetable oils, *J. Agric. Food. Chem.* 56 (2008) 8919–8925.
- Global Market for Lubricating Oils and Greases to Reach 10.9 Billion Gallons by New Reports by Global Industry Analysts, Inc., 2012, http://www.prweb.com/releases/lubricatingoils/lubricants_reases/prweb9351336.htm, (Accessed 29 November 2016).
- H.A. Hanmid, R. Yunus, U. Rashid, T.S.Y. Choong, A.H. Al-Muhtaseb, Synthesis of palm oil-based trimethylolpropane ester as potential biolubricant: chemical kinetics modelling, *Chem. Eng. J.* 200 (2012) 532–540.
- S. Gryglewicz, M. Muszynski, J. Nowicki, Enzymatic synthesis of rapeseed oil-based lubricants, *Ind. Crop. Prod.* 45 (2013) 25–29.
- P. Nagendramma, S. Kaul, Development of ecofriendly/biodegradable lubricants: an overview, *Renew. Sust. Energy Rev.* 16 (2012) 764–774.
- B. Wilson, Lubricants and functional fluids from renewable sources, *Ind. Lubr. Tribol.* 50 (1998) 6–15.
- J.R. Steven, Synthetics, mineral oils, and bio-based lubricants: chemistry and technology, in: R.L. Rudnick (Ed.), *Chemical Industries*, CRC Press, Boca Raton, 2006, pp. 47–74.
- R. Yunus, A. Fakhru'l-Razi, T.L. Ooi, D.R.A. Biak, S.E. Iyuke, Kinetics of transesterification of palm-based methyl esters with trimethylolpropane, *J. Am. Oil Chem. Soc.* 81 (2004) 497–503.
- Y.Y. Linko, X.Y. Wu, Biocatalytic production of useful esters by two forms of lipase from *candida rugose*, *J. Chem. Technol. Biotechnol.* 56 (1996) 163–170.
- E. Uosukainen, Y.Y. Linko, M. Lämsä, T. Tervakangas, P. Linko, Transesterification of trimethylolpropane and rapeseed oil methyl ester to environmentally acceptable lubricants, *J. Am. Oil Chem. Soc.* 75 (1998) 1557–1563.
- M. Di Serio, R. Tesser, M. Dimiccoli, F. Cammarota, M. Nastasi, E. Santacesaria, Synthesis of biodiesel via homogeneous lewis acid catalyst, *J. Mol. Catal. A: Chem.* 239 (2005) 111–115.
- M.H. Zong, Z.Q. Duan, W.Y. Lou, T.J. Smith, H. Wu, Preparation of a sugar catalyst and its use for highly efficient production of biodiesel, *Green Chem.* 9 (2007) 434–437.
- Z.Z. Yang, W.L. Xie, Y. Zuo, Application in transesterification of oil and fat via heterogeneous base catalysts, *Cereal Oil* 7 (2006) 13–16.
- L.J. Gao, G.Y. Teng, G.M. Xiao, R.P. Wei, Biodiesel from palm oil via loading KF/Ca-Al hydrotalcite catalyst, *Biomass Bioenergy* 34 (2010) 1283–1288.
- X. Deng, Z. Fang, Y.H. Liu, C.L. Yu, Production of biodiesel from jatropha oil catalyzed by nanosized solid basic catalyst, *Energy* 36 (2011) 777–784.
- H. Liu, L.Y. Su, F.F. Liu, C. Li, U.U. Solomon, Cinder supported K₂CO₃ as catalyst for biodiesel production, *Appl. Catal. B: Environ.* 106 (2011) 550–558.
- W.L. Xie, L.L. Zhao, Heterogeneous CaO–MoO₃–SBA-15 catalysts for biodiesel production from soybean oil, *Energy Convers. Manag.* 79 (2014) 34–42.
- M. Farooq, A. Ramli, D. Subbarao, Biodiesel Production from waste cooking oil using bifunctional heterogeneous solid catalysts, *J. Clean Prod.* 59 (2013) 131–140.
- N.P. Asri, S. Machmudah, Suprapto Wahyudiono, K. Budikarjono, A. Roesyadi, M. Goto, Palm oil transesterification in sub- and supercritical methanol with heterogeneous base catalyst, *Chem. Eng. Process.* 72 (2013) 63–67.
- G. Teng, L. Gao, G. Xiao, H. Liu, J. Lv, Biodiesel preparation from jatropha curcas oil catalyzed by hydrotalcite loaded with K₂CO₃, *Appl. Biochem. Biotechnol.* 162 (2010) 1725–1736.
- Z. Zhang, X. Ma, Y. Wang, R.A. Yan, M.M. Liu, Production of monoacylglycerols from fully hydrogenated palm oil catalyzed by hydrotalcite loaded with K₂CO₃, *Chem. Eng. Commun.* 202 (2015) 585–592.
- Y. Wang, S. Ma, L.L. Wang, S.Z. Tang, W.W. Riley, M.J.T. Reaney, Solid superacid catalyzed glycerol esterification of free fatty acids in waste cooking oil for biodiesel production, *Eur. J. Lipid Sci. Technol.* 114 (2012) 315–324.
- E.P. Wang, X. Ma, S.Z. Tang, R.A. Yan, Y. Wang, W.W. Riley, M.J.T. Reaney, Synthesis and oxidative stability of trimethylolpropane fatty acid triester as a biolubricant base oil from waste cooking oil, *Biomass Bioenergy* 66 (2014) 371–378.
- Y. Wang, E.P. Wang, S.Z. Tang, Z. Zhang, M.J.T. Reaney, Synthesis of trimethylolpropane fatty acid triester as biolubricant from palm-based methyl esters and trimethylolpropane, *J. Chin. Cereals Oils Assoc.* 28 (2013) 27–32.
- T.S. Chang, H. Masood, R. Yunus, U. Rashid, T.S.Y. Choong, D.R.A. Biak, Activity of calcium methoxide catalyst for synthesis of high oleic palm oil based trimethylolpropane triesters as lubricant base stock, *Ind. Eng. Chem. Res.* 51 (2012) 5438–5442.
- I. Alexandra, I.Z. Mohamed, K. Charles, Interfacial chemistry in the preparation of catalytic potassium-modified, *J. Chem. Soc. Faraday Trans.* 89 (1993) 2527–2536.
- W.L. Xie, H. Peng, L.G. Chen, Transesterification of soybean oil catalyzed by potassium loaded on alumina as a solid-base catalyst, *Appl. Catal. A: Gen.* 300 (2006) 67–74.
- I. Lukic, J. Krstic, D. Jovanovic, D. Skala, Alumina/silica supported K₂CO₃ as a catalyst for biodiesel synthesis from sunflower oil, *Bioresour. Technol.* 100 (2009) 4690–4696.
- W.L. Xie, H.T. Li, Alumina-supported potassium iodide as a heterogeneous catalyst for biodiesel production from soybean oil, *J. Mol. Catal. A: Chem.* 255 (2006) 1–9.
- D.M. Alonso, R. Mariscal, R. Moreno-Tost, M.D.Z. Poves, M.L. Granados, Potassium leaching during triglyceride transesterification using K/c-Al₂O₃ catalysts, *Catal. Commun.* 8 (2007) 2074–2080.
- G. Busca, V. Lorenzelli, Infrared spectroscopic identification of species arising from reactive adsorption of carbon oxides on metal oxide surfaces, *Mater. Chem.* 7 (1982) 89–126.
- H.A. Al-Abadleh, H.A. Al-Hosney, V.H. Grassian, Oxide and carbonate surfaces as environmental interfaces: the importance of water in surface composition and surface reactivity, *J. Mol. Catal. A: Chem.* 228 (2005) 47–54.
- F.F. Chen, F. Yang, G.H. Wang, W. Li, Calcined Zn/Al hydrotalcites as solid base catalysts for glycolysis of poly (ethylene terephthalate), *J. Appl. Polym. Sci.* 131 (2014).
- I.Z. Alexandra, Formation of carboxy species at CO/Al₂O₃ interfaces. Impacts of surface hydroxylation, potassium alkalinization and hydrogenation as assessed by in situ FTIR spectroscopy, *Phys. Chem. Chem. Phys.* 6 (2004) 2502–2512.
- F. Cavaní, F. Trifiro, A. Vaccari, Hydrotalcite-type anionic clays: preparation, properties and applications, *Catal. Today* 11 (1991) 173–301.
- D.G. Cantrell, L.J. Gillie, A.F. Lee, K. Wilson, Structure-reactivity correlations in MgAl hydrotalcite catalysts for biodiesel synthesis, *Appl. Catal. A: Gen.* 287 (2005) 183–190.
- M.G. Alvarez, A.M. Segarra, S. Contreras, J.E. Sueiras, F. Medina, F. Figueras, Enhanced use of renewable resources: transesterification of glycerol catalyzed by hydrotalcite-like compounds, *Chem. Eng. J.* 161 (2010) 340–345.

- [38] J.F.P. Gomes, J.F.B. Puna, L.M. Goncalves, J.C.M. Bordado, Study on the use of MgAl hydrotalcites as solid heterogeneous catalysts for biodiesel production, *Energy* 36 (2011) 6770–6778.
- [39] T. Wan, P. Yu, S. Gong, Q. Li, Y. Luo, 2008. Application of KF/MgO as a heterogeneous catalyst in the production of biodiesel from rapeseed oil, *Korean J. Chem. Eng.* 25 (2008) 998–1003.
- [40] Y.H. Li, F.X. Qiu, D.Y. Yang, X.H. Li, P. Sun, Preparation, characterization and application of heterogeneous solid base catalyst for biodiesel production from soybean oil, *Biomass Bioenergy* 35 (2011) 2787–2795.
- [41] M. Tu, J. Shen, Y. Chen, Microcalorimetric studies of Zn-Al mixed oxides obtained from hydrotalcite-type precursors, *J. Therm. Anal. Calorim.* 58 (1999) 441–446.
- [42] C.J. Sun, F.X. Qiu, D.Y. Yang, B. Ye, Preparation of biodiesel from soybean oil catalyzed by Al-Ca hydrotalcite loaded with K_2CO_3 as heterogeneous solid base catalyst, *Fuel Proces. Technol.* 126 (2014) 383–391.
- [43] L. Čapek, M. Hájek, P. Kutálek, L. Smoláková, Aspects of potassium leaching in the heterogeneously catalyzed transesterification of rapeseed oil, *Fuel* 115 (2014) 443–451.
- [44] P. Liu, M. Derchi, E.J.M. Hense, Promotional effect of transition metal doping on the basicity and activity of calcined hydrotalcite catalysts for glycerol carbonate synthesis, *Appl Catal. B: Environ.* 144 (2014) 135–143.